Proc. Vth International Workshop, Advances in Signal Processing for Non Destructive Evaluation of Materials
Québec City (Canada),2-4 Aug. 2005. © X. Maldague ed., É. du CAO (2006), ISBN 2-9809199-0-X

Usability of ECT for Quantitative and Qualitative Characterization of Trickle-Bed Flow Dynamics Experiencing Filtration Conditions

Cristian Tibirna[1], David Edouard[2], André Fortin[1], Faïçal Larachi[2]

[1] *GIREF, Université Laval, Québec, Canada;* [2] *Département de Génie Chimique, Université Laval, Québec, Canada*

Abstract

This work investigates the pros and cons of using the Electrical Capacitance Tomography (ECT) for imaging and quantitative characterization of flow dynamics in a four-phase trickle-bed reactor. ECT use is increasing in non-invasive imaging thanks to its low cost and convenience compared to nuclear ionizing, non-ionizing and other tomography methods. Yet, ECT has low spatial resolution, lack of multi-modality and difficult image reconstruction. The flow dynamics that establish in a four-phase trickle-bed system are complex and prone to instability. This work sets to determine in what measure ECT cat precisely capturing steady-state flow features and unsteady situations: plugging, preferential flowing etc. Many image reconstruction algorithms are tested in the light of the trickle-bed reactor characteristics.

Keywords: electrical capacitance tomography, trickle-bed reactor, multiphase process, image reconstruction, inverse problem.

1. Introduction

The present work is part of a broader project whose main goal is to find ways for increasing the lifetime of catalyst beds in the trickle-bed catalytic reactors used in the hydro-treatment of some oil fractions. The speed at which the catalyst bed is clogging with mineral deposits needs to be reduced. In order to reach this goal, a better understanding of the flow dynamics and clogging physics in trickle-bed reactors is necessary. This requires, among others, to establish a reliable non-intrusive investigation method which can provide better experimental information about flowing and clogging, so that new models can be based on.

Athabasca bitumen contains finely dispersed particles of clay solids, some of which are carried into the gas oil fraction during initial stages of distillation. The distilled fraction has to go to a catalytic hydro-treatment reactor, usually a *trickle-bed reactor*. Suspended particles still present in this fraction are thus a nuisance.

Filtration prior to the reactor bed can remove particles larger than *e.g.*, 25 mm. Fine particles (usually called *fines*) still remain in the fraction. These accumulate in the reactor significantly over many months of operation, by depositing throughout the catalyst bed. This increases the pressure drop to a point where the plant has to be shut down and the catalyst replaced. When this occurs before the end of designed activity life of the catalyst, the operation costs rise unnecessarily.

The interstitial velocity of liquid in the trickle-bed reactor has an important influence on the mechanisms of deposition of fine solids that occurs in the bed of catalyst pellets. The complex mechanisms of the process of fines deposition and pressure drop in the trickle-bed reactor is understood only partially. An effort for finding a good physico-mathematical model for these mechanisms is under way [1]. The validation of this model requires methods of experimental investigation that are both precise and non-intrusive.

Based on previous work focused on three-phase trickle-bed reaction [2], the Electrical Capacitance Tomography (ECT) is pondered in this work as a plausible non-intrusive method of investigation for the deposition mechanisms and flow dynamics in the four-phase trickle-bed reactor. The current investigation focuses on a number of aspects, both favorable and unfavorable, of the ECT as used for non-intrusive imaging of the type of processes mentioned above.

2. Experimental setup

The main elements of the simple experimental setup are schematically represented at *figure 1*. The catalyst bed with a diameter of 57 mm and a height of 920 mm is formed of spherical alumina pellets with a mean diameter of 2.7 mm. The porosity of the catalyst bed was measured at 32%.

A solution of kaolin fines in kerosene, continuously stirred, is sent with controlled flow rates to the top of the packed column. The kaolin was selected because it is the major component of clay minerals found in the Athabasca oil sands. Kerosene was selected due to its similarity – notably given its chemical stability and its low vapor pressure – to the hydrocarbon streams submitted to hydro-treating.

Air and liquid solution are injected through a diffuser for even distribution in the catalyst bed. Liquid flow rate is constant at 0.001 ml/s. The following gas flow rates are used: 0.045 ml/s, 0.123 ml/s, 0.185 ml/s and 0.216 ml/s. A differential pressure sensor measures the pressure drop between the top and the bottom of the packed bed. The tank at the exit of the column allows to store and stir magnetically the output suspension. The inlet concentration of kaolin can be maintained constant by time intervals or varied permanently (see Edouard and Larachi [3]).

The concentration of the kaolin suspension in kerosene is measured periodically in the feed (C_{in}) and in the exit flow (C_{out}) with a Hach 2100P turbidimeter. The maximum concentration was about 1.8 g/l.

For deposition to occur, the suspension of kaolin in kerosene has to be stable. The particle agglomerates should not exceed 10 μm and the use of a surfactant is mandatory. Cetyltrimethylammonium bromide ($C_{19}H_{42}NBr$), also known as CTAB, was added to the kerosene, in proportions of 5% of the mass of kaolin (see [3]).

The ECT equipment used is a PTL300E with a DAM200E sensor controller, from Process Tomography Limited. The sensor has an internal diameter of 63.5 mm, with two adjacent planes of 12 electrodes. The two rows of measurement electrodes are 50 mm high with guard electrodes of 38 mm height placed immediately above and below. The role of the guard electrodes is to confine the electric field measured by the active electrodes to a horizontal section of the reactor. The geometry of sensor's electrodes is given in *figure 2*. The tomograph is controlled from a computer program which also serves for collecting the measurements.

The ECT sensor can be placed at three fixed positions along the column. The top of the sensor is at 330 mm, 580 mm and 860 mm respectively from the bottom of the catalyst bed. The tomographic images obtained at these positions allow to detect differences in the flow dynamics and deposit profiles that might vary with the height of the catalyst bed.

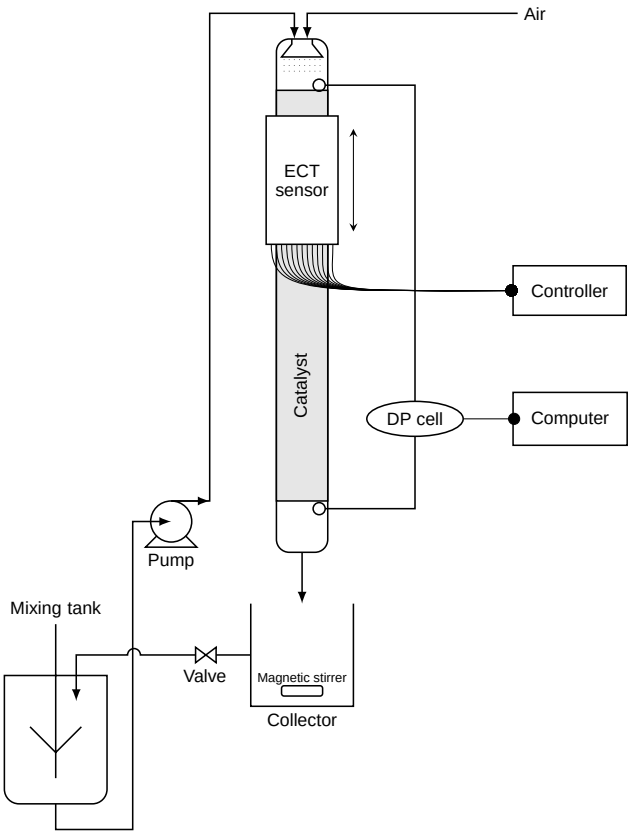

Figure 1: Schematic representation of the experimental setup

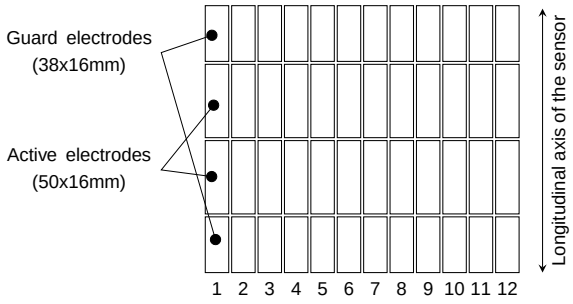

Figure 2: Geometry of the electrodes used in the ECT sensor

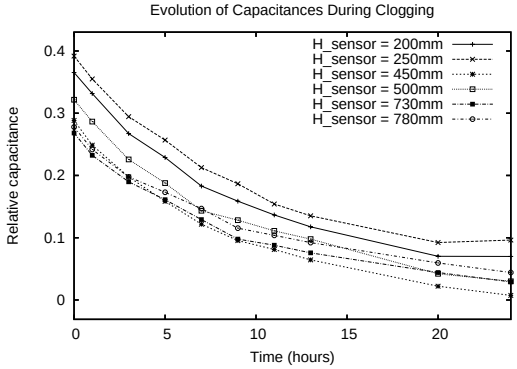

Figure 3: Time variation of the mean relative permittivity in the trickle-bed reactor

3. Advantages and disadvantages of using ECT

ECT is based on dielectric properties of materials (thus well suited for chemical processes) and is non-intrusive (electrodes are placed *on the outside* of the reactor wall)[1]. It is also fast and it is not as expensive as *hard field tomography*[2] while being essentially harmless for human operators and environment. ECT equipment and operation is inexpensive when compared with other non-intrusive tomography methods and this is another major advantage of the technology.

[1] Electrodes can also be placed on the inside of the reactor wall; the essential is that in both configurations, the sensing part of the ECT technology in no way obstructs the hydrodynamics of the sensed system (reactor).

[2] X-ray, γ-ray, nuclear resonance tomographies and so on.

3.1. High speed of ECT allows for detailed characterizations

The current ECT equipment allows for up to 100 tomograms per second to be recorded. The clogging experiment usually goes in about 30 hours from a completely clean catalyst bed to a stable, non-filtering clogging state.

In a first stage, the experiment has been designed to record series of three tomograms, at 330, at 580 and at 860 mm on the height of the catalyst bed (900 mm) once at each 2 hours. This allowed to identify the evolution tendencies of the bed permittivities in the three distinct sections of the reactor (see *figure 3*). Full reactor scans were also performed manually, which allowed to observe liquid and gas flow patterns.

In the next stage of the project, a precise automated ECT scanning mechanism will eventually be put in place, which will allow for full 3D reactor scans to be obtained at given time intervals. This will allow for collecting more detailed data and probably for better differentiation of localized phenomena.

3.2. ECT image reconstruction is a difficult inverse problem

The electric field in ECT is embarrassingly non-linear. This introduces very much indetermination in the reconstruction of the tomograms. The reconstruction itself implies the resolution of an inverse problem of difficult nature, mathematically and numerically.

The fundamental transfer equation which describes the electric field in a plane section of the ECT sensor is a Poisson equation [4]:

$$\nabla \cdot (\varepsilon_0 \varepsilon(x,y) \nabla \phi(x,y)) = 0 \tag{1}$$

where ε_0 is the absolute permittivity of vacuum, ε is the relative permittivity of the material found in the electric field and ϕ is the representation of the electric field. From this equation is deduced the measure of the capacitance between two electrodes [5]:

$$C = -\frac{1}{\Delta V} \iint_{\Gamma} \varepsilon_0 \varepsilon(x,y) \nabla \phi(x,y) d\Gamma \tag{2}$$

After a derivation, linearization and normalization, the best known equation of ECT results:

$$\lambda = Sg \quad \text{or} \quad g = S^{-1}\lambda \tag{3}$$

where λ is the normalized vector of capacitances (of size M), g is the vector of permittivities at each pixel of the zone of measurement (of size N) and S is the sensitivity matrix (of size $M \times N$).

The problem is to determine the unknown g (distribution of permittivities in the system) from the S measured in precise experimental conditions and given a λ measured for the unknown g. This is a badly posed problem because $M \ll N$, hence S is non-invertible.

3.3. Image reconstruction algorithms

Many image reconstruction algorithms are presented in the literature [5, 6] and they are intended for systems containing large features (like gas bubbles) in rapid motion (as in gas fluidization reactors). Very brief descriptions follow.

3.3.1. Non-iterative algorithms

The **Linear Back Projection (LBP)** is the most largely used image reconstruction algorithm for ECT. It is borrowed from the hard field tomography. The fundamental equation of this algorithm is:

$$\hat{g} = \frac{S^T \lambda}{S^T u_\lambda} \tag{4}$$

where u_λ is a unit vector with the same dimension as λ.

The main advantage of LBP is its simplicity, which also makes it fast and easy to perform by a computer. Thus image reconstruction using this algorithm is very fast. The downside consists in the really poor quality of the reconstructed image. An impairing smoothing/smearing occurs in the reconstructed image when compared with the real image.

The **Single Value Decomposition (SVD)** algorithm – and its truncated and filtered versions – is mathematically described as:

$$S = U\Sigma V^T \quad \text{then} \quad \hat{g} = V\Sigma^{-1}U^T\lambda \tag{5}$$

These algorithms offer very interesting image quality for the low computing costs that they imply.

The **Tikhonov regularization** method [7] means:

$$\hat{g} = (S^TS + \mu I)^{-1}S^T\lambda \tag{6}$$

This method seems to be difficult to control and requires arbitrarily chosen parameters (μ).

3.3.2. Iterative algorithms

The **Iterative Tikhonov** method performs, at each iteration, a Tikhonov regularization:

$$\hat{g}_{k+1} = \hat{g}_k - (S^TS + \mu I)^{-1}S^T(S\hat{g}_k - \lambda) \tag{7}$$

The **Landweber and Projected Landweber** methods [8, 9] are iterative algorithms inspired from the research on correcting photographic images.

$$\hat{g}_{k+1} = \hat{g}_k - \alpha S^T(S\hat{g}_k - \lambda) \tag{8}$$

Until very recently, the Landweber algorithm was considered the *"state of the art"* in ECT image reconstruction. Unfortunately it has rather severe numerical inconveniences, related to the necessity of using a number of arbitrary parameters as well as lacking a reliable iteration stop criterium.

The **Simultaneous Iterative Reconstruction Technique (SIRT)** is also inspired from the hard field tomography.

$$\hat{g}_{k+1} = \hat{g}_k - \beta S^T \frac{S\hat{g}_k - \lambda}{\operatorname{diag} SS^T} \tag{9}$$

It is very similar to the Landweber method. Its main advantage resides in the way it is often implemented: β is a weighting vector (allowing to give discriminate importance to specific parts of the measured capacitances vector).

3.3.3. Image reconstruction results

All these classic algorithms were implemented in a programming framework based on the Python programming language and using Python's high performance *Numeric* library. The algorithms were then applied to synthetic images obtained by FEM simulations realized with a special code based on the *MEF*++ library developed by the GIREF research group at Laval University, Québec. A graphical comparison of reconstruction results obtained with these algorithms is given at *figure 4*. The goals of the exercise were:

- to test these algorithms for systems with diffuse features (like diffuse concentration distributions of system components);
- to be able to choose the most convenient algorithm for reconstruction of images from this kind of quasi-static systems;
- to select the better working parameters and iteration stop criteria.

Figure 4 shows how different image reconstruction algorithms behave given a particular original image (phantom). One essential observation is that images of distinct objects (like spots, bars and multiple spots) are relatively well reconstructed; when it comes to annular or quadratic profiles (like those shown in the last three lines in *figure 4*), the reconstructed images don't allow to distinguish essentially different original permittivity setups. The most disturbing is the difficulty to distinguish between annular and parabolic setups. It is almost equally possible for such situations to occur in a plugging trickle-bed reactor and thus the imaging technology we choose should enable us to differentiate them. This could become an important handicap in using ECT for trickle-bed reactors imaging.

3.3.4. Process simulation using *MEF*++

The Finite Element Method library *MEF*++, developed by GIREF at Laval University, was used as a tool-chain for the development of a simulator for the dispersion of the electric field inside a system characterized by a non-homogeneous permittivity distribution. Thanks to the high quality of the MEF++ library, only marginal effort was required for the creation of the simulator code. More notable, special routines were created for the integration of the electric field on surfaces present inside the simulated domain.

More energy was required for the creation of a large number of Finite Element meshes that served as supports for the simulations and for precise image reconstruction. Examples of such meshes are given at *figure 5*. The mixed structured/non-structured grid in *figure 5(b)* is particularly difficult to obtain with the meshing tools available today.

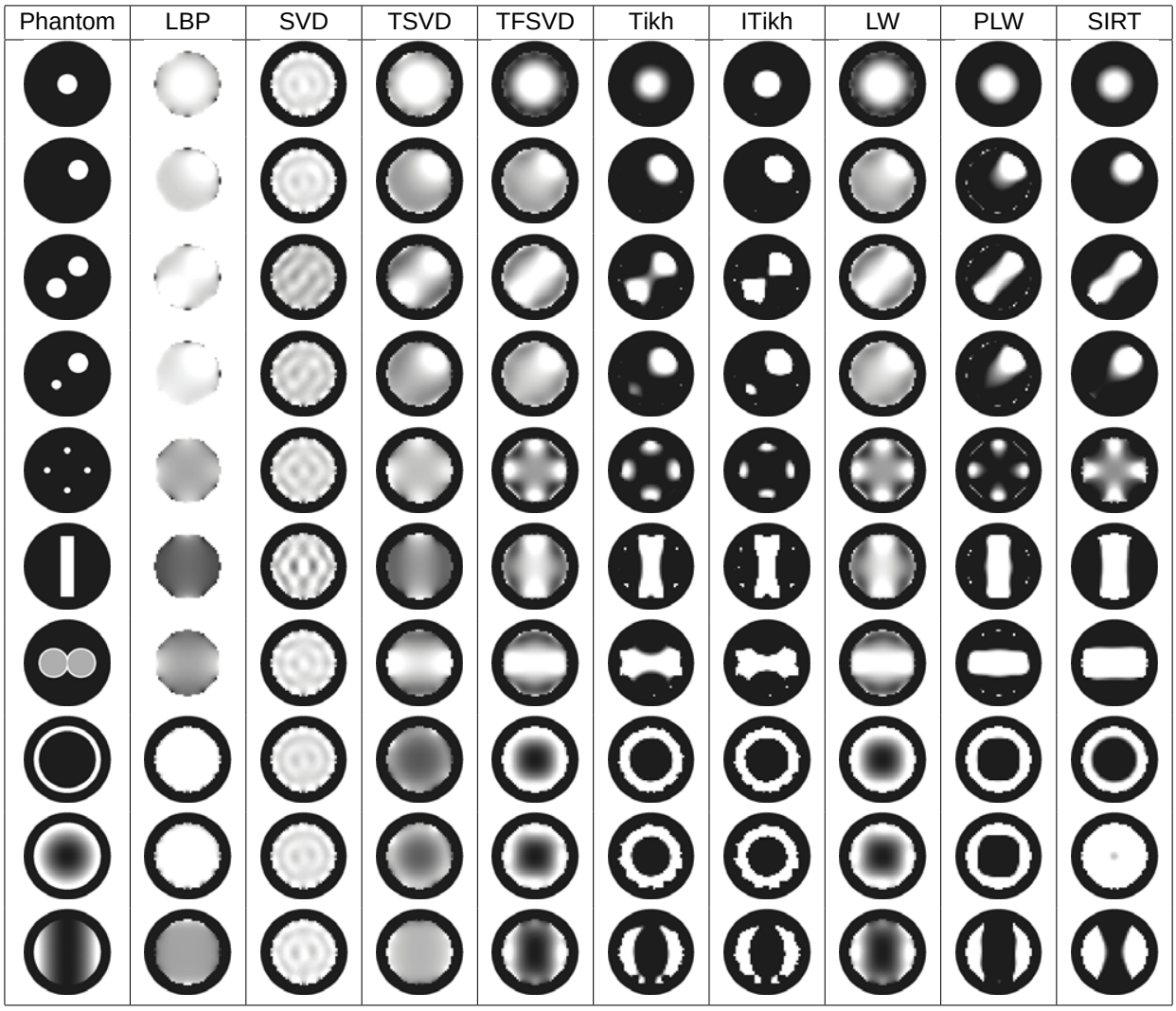

Figure 4: Comparative results of classic image reconstruction algorithms. Algorithms: LBP = Linear Back Projection; (TF)SVD = (Truncated Filtered) Single Value Decomposition; (I)Tikh = (Iterative) Tikhonov; (P)LW = (Projected) Landweber; SIRT = Simultaneous Iterative Reconstruction Technique

3.3.5. Four-phases system

The four-phases trickle-bed reactor used in our setup experiments, for the study of plugging, contains the following phases: solid (catalytic bed of γ-alumina: $\varepsilon_s = 4.5 \times \varepsilon_0$[3]); liquid (kerosene: $\varepsilon_l = 2.2 \times \varepsilon_0$); gas (air: $\varepsilon_g \approx 1.0 \times \varepsilon_0$); suspension of solid fines (kaolin: $\varepsilon_f = 5.0 \times \varepsilon_0$ in kerosene). There is also the surfactant (CTAB: $\varepsilon_f = 36.0 \times \varepsilon_0$). The fines are initially suspended in the liquid phase, but are then depositing on the solid catalyst bed. They are thus forming porous layers in which the pores can be filled either with liquid or with gas. This complex structure puts strains on the detection limits of ECT, as each of these phases has a different relative permittivity contributing to the mean permittivity of the system.

ECT allows for measuring permittivities interpolated linearly between the lowest and the highest values present in the system and fixed by calibration. The literature also presents techniques for imaging objects of three distinct permittivities. Fitting a tomogram to the kind of smooth distribution of permittivities that is seen in trickle-bed reactors requires further refinement of the mathematical models and reconstruction algorithms of ECT.

[3] $\varepsilon_0 = 8.8524 \times 10^{-12}$ F/m is the absolute permittivity of vacuum.

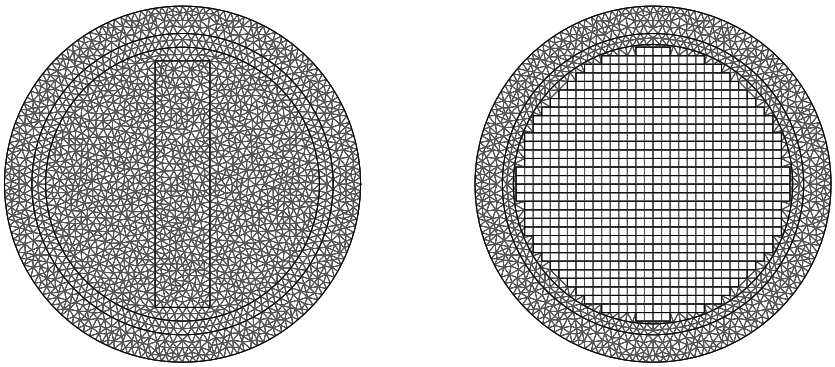

(a) Mesh for simulation (b) Mesh for image reconstruction

Figure 5: Examples of FEM meshes used in ECT

4. Conclusions

ECT is an attractive imaging method to be used for trickle-bed reaction processes. It is fast and inexpensive. It is non-intrusive and this constitutes its main advantage.

The algorithms presented in the literature for ECT image reconstruction are well adapted for detection of objects. Images of smooth composition distributions are difficult to reconstruct. We determined that for this latest kind of images, truncated and filtered SVD (TFSVD) and Landweber methods are the most appropriate. More advanced methods, based on FEM or on neural networks, must be tried.

The technologies involved in ECT are complex and still require improvement and refinement. Work is in course for improving the calibration methodologies and for devising ECT scannings of full reactor length.

In its current state, ECT is applicable to trickle-bed reactor characterizations mostly as a diagnostic technique. Its use for quantitative measurements will become possible after the improvement of reconstruction techniques for smooth permittivity distribution images.

References

[1] Iliuta, I., Larachi, F. and Grandjean, B. *Fines Deposition Dynamics in Gas-Liquid Trickle-Flow Reactors*. AIChE Journal, (49), 2003, pp. 485–495

[2] Reinecke, N. and Mewes, D. *Tomographic imaging of trickle-bed reactors*. Chemical Engineering Science, 51(10), 1996, pp. 2131–2138

[3] Edouard, D. and Larachi, F. *The Role of Gas Phase in Deposition Dynamics of Fine Particles in Trickle-Bed Reactors*. 2005. In preparation

[4] Xie, C., Huang, S., Hoyle, B., Thorn, R., Lenn, C., Snowden, D. and Beck, M. *Electrical capacitance tomography for flow imaging: system model for development of image reconstruction algorithms and design of primary sensors*. Circuits, Devices and Systems, IEE Proceedings G, 139, 1992, pp. 89–98

[5] Yang, W. Q. and Peng, L. *Image reconstruction algorithms for electrical capacitance tomography*. Measurement Science and Technology, 14(1), 2003, p. R1

[6] Øyvind Isaksen. *A review of reconstruction techniques for capacitance tomography*. Meas. Sci. Technol, (7), 1996, pp. 325–337

[7] Tikhonov, A. N. and Arsenin, V. Méthodes de résolution de problèmes mal posés. MIR, Moscou, 1976. Translated from russian

[8] Liang, L. and Xu, Y. *Adaptive Landweber Method to Deblur Images*. IEEE Signal Processing Letters, 10(5), 2003, pp. 129–133

[9] Yang, W. Q., Spink, D. M., York, T. A. and McCann, H. *An image-reconstruction algorithm based on Landweber's iteration method for electrical-capacitance tomography*. Measurement Science and Technology, 10(11), 1999, p. 1065